

# Selective Imaging of HClO in the Liver Tissue In Vivo Using a Near-infrared Hepatocyte-specific Fluorescent Probe

Xu Jia,<sup>[a]</sup> Chao Wei,<sup>\*[a]</sup> Zimeng Li,<sup>[a]</sup> Liyan Liu,<sup>[b]</sup> Mei Wang,<sup>[a]</sup> Pingzhu Zhang,<sup>[a]</sup> and Xiaoliu Li<sup>\*[a]</sup>

**Abstract:** Liver injury is typified by an inflammatory response. Hypochlorous acid (HClO), an important endogenous reactive oxygen species, is regarded as a biomarker associated with liver injury. Near-infrared (NIR) fluorescent probes with the advantage of deep tissue penetrating and low auto-fluorescence interference are more suitable for bioimaging in vivo. Thus, in this work, we designed and synthesized a novel NIR hepatocyte-specific fluorescent probe named **NHF**. The probe **NHF** showed fast response (<3 s), large spectral variation, and good selectivity to trace HClO in buffer

solution. By employing *N*-acetylgalactosamine (GalNAc) as the targeting ligand, probe **NHF** can be actively delivered to the liver tissue of zebrafish and mice. It is important that probe **NHF** is the first NIR hepatocyte-specific fluorescent probe, which successfully visualized the up-regulation of endogenous HClO in the oxygen-glucose deprivation/reperfusion (OGD/R) model HepG2 cells and dynamically monitored APAP-induced endogenous HClO in the liver tissue of zebrafish and mice.

## Introduction

Hypochlorous acid is a colorless liquid with irritant odor. Because of its strong oxidation, hypochlorous acid/hypochlorite (HClO/CIO<sup>-</sup>) has been widely used as an effective disinfectant for indoor air, drinking water, fruits, vegetables, and tableware.<sup>[1]</sup> Thus, excess ClO<sup>-</sup> residue in drinking water and the environment is harmful to human beings. Besides, HClO is an important reactive oxygen species (ROS), which is mainly from the peroxidation reaction of H<sub>2</sub>O<sub>2</sub> and chloride ion (Cl<sup>-</sup>) with the assistance of the heme myeloperoxidase.<sup>[2]</sup> Endogenous HClO is involved in regulating various physiological and pathological processes.<sup>[3]</sup> However, the imbalance of endogenous HClO will cause cardiovascular diseases,<sup>[4]</sup> inflammatory diseases,<sup>[5]</sup> atherosclerosis,<sup>[6]</sup> liver injury,<sup>[7]</sup> cancer,<sup>[8]</sup> etc. Among them, liver injury is a common disease that cannot be ignored, which is typified by an inflammatory response. HClO, an important endogenous ROS, is regarded as a biomarker associated with liver injury. Based on the above importance of HClO, the effective detection of HClO in the liver *in vivo* is of vital importance.

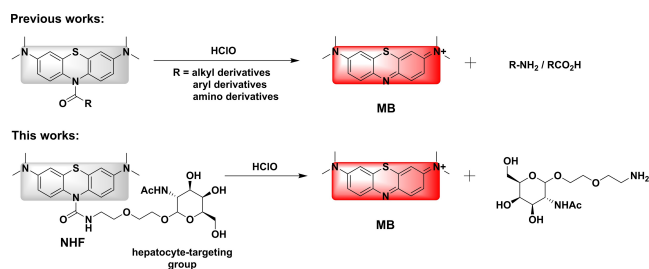
It is accepted that fluorescent probe method is the most effective assay for HClO detection *in vitro* and *in vivo* because of its easy preparation and operation, high selectivity and sensitivity, non-destructive to tissues, and high-fidelity imaging.<sup>[9]</sup> Although many fluorescent HClO probes have been reported, there are some problems with selective detection of hypochlorous acid in liver *in vivo*. The first is the selectivity of the probe. Most fluorescent probes have been designed based on the strong oxidizing property of HClO.<sup>[10]</sup> So, some reactive species having comparable oxidizability with HClO, such as peroxynitrite (ONOO<sup>-</sup>), might interfere with the detection of HClO.<sup>[11]</sup> Second, the NIR fluorescent probe shows deep photon penetration, reduced photo damage and minimized background fluorescence, which is more suitable for monitoring the production and metabolism of endogenous HClO *in vivo*.<sup>[12]</sup> But, NIR fluorescent probe for HClO detection *in vivo* is still insufficient. Third, the up-regulation of endogenous HClO is associate with liver diseases. Unfortunately, the existing fluorescent probes are not yet available for *in situ* imaging of HClO in the liver *in vivo*.<sup>[13]</sup> Therefore, it is necessary to construct an ideal hepatocyte-specific probe with NIR emission wavelength and high selectivity to HClO (Table S1).

Recently, methylene blue (MB) based NIR fluorescent probes have been developed for rapid detection of HClO with high selectivity *in vitro* and *in vivo* (Scheme 1a).<sup>[14]</sup> We reported two GalNAc modified probes that can be specifically delivered to the liver *in vivo* due to the specific receptor-ligand interaction.<sup>[15]</sup> Herein, by properly linking reduced MB to GalNAc, the first NIR hepatocyte-specific HClO fluorescent probe (**NHF**) was designed and synthesized (Scheme 1b). As expected, probe **NHF** exhibited fast fluorescence response (<3 s) and excellent selectivity towards HClO over other various ROS. Cell imaging experiments showed that probe **NHF** could be actively delivered to hepatocytes and used for monitoring the production of endogenous HClO in OGD/R HepG2 cells. More

[a] X. Jia, Dr. C. Wei, Z. Li, Dr. M. Wang, Prof. Dr. P. Zhang, Prof. Dr. X. Li  
 Key Laboratory of Medicinal Chemistry and  
 Molecular Diagnosis (Ministry of Education)  
 Key Laboratory of Chemical Biology of Hebei Province  
 College of Chemistry and Environmental Science  
 Hebei University  
 Wusi Dong Road 18, Baoding 071002 (P. R. China)  
 E-mail: weichao@hbu.edu.cn  
 lixl@hbu.cn

[b] L. Liu  
 Medical Comprehensive Experimental Center  
 Hebei University  
 East Road Yuhua 342, Baoding 071000 (P. R. China)

Supporting information for this article is available on the WWW under  
<https://doi.org/10.1002/asia.202100476>



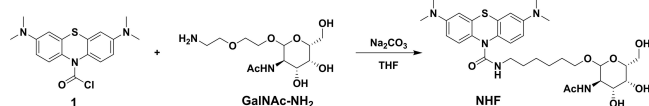
Scheme 1. a) the previous work. b) The design strategy of this work.

importantly, probe **NHF** was successfully applied to monitor acetaminophen-induced fluctuations of endogenous HClO levels in the liver of zebrafish and mice.

## Results and Discussion

**Synthesis and identification of probe NHF.** Probe **NHF** was easily obtained by the amidation reaction between compound **1** and GalNAc-NH<sub>2</sub> according to the synthetic route as shown in Scheme 2. The structure of probe **NHF** was identified by <sup>1</sup>H NMR, <sup>13</sup>C NMR, and HRMS (Figure S1-S3).

**Spectroscopic Properties.** By modification with polyhydroxy carbohydrates, probe **NHF** displayed good water solubility. Thus, the absorption and fluorescence spectra were first respectively recorded in presence of different concentrations of HClO in PBS (pH=7.4, 20 mM). As shown in Figure 1a and



Scheme 2. The synthesis route of probe **NHF**.

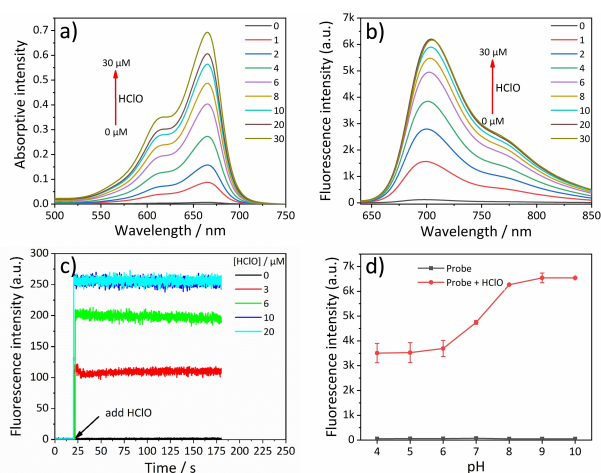


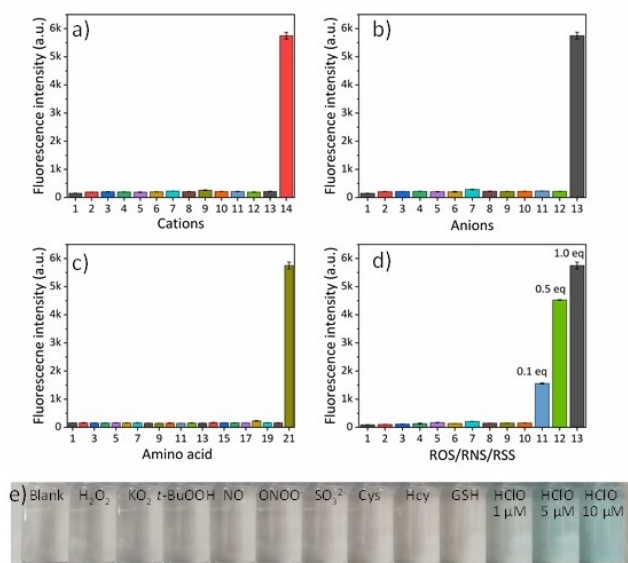
Figure 1. (a) Absorption and (b) fluorescence spectra of **NHF** (10  $\mu\text{M}$ ) with different concentrations of HClO (1–30  $\mu\text{M}$ ). (c) Time-dependent fluorescence intensity ( $F_{700\text{ nm}}$ ) of probe **NHF** (10  $\mu\text{M}$ ) in presence of HClO (0, 3, 6, 10, 20  $\mu\text{M}$ ). (d) The fluorescence intensity ( $F_{700\text{ nm}}$ ) of probe **NHF** (10  $\mu\text{M}$ ) with and without HClO (100  $\mu\text{M}$ ) in PBS with different pH values (4.0–10.0).

Figure 1b, probe **NHF** is a near-infrared probe, its maximum absorption and emission peaks are close to 664 nm and 700 nm, respectively. After adding HClO, obvious spectral enhancement appeared for absorption and fluorescence spectra. By fitting the absorptive intensities at 664 nm with the HClO concentration (0–8  $\mu\text{M}$ ), a good linear relationship ( $y=0.0075+0.0603x$ ,  $R^2=0.999$ ) was appeared (Figure S4). To obtain the detection limit, we further recorded the emission intensity of probe **NHF** after reaction with a small amount of HClO (0–1.0 equiv). By fitting the concentration of HClO added and the intensities of probe **NHF** at 700 nm, the detection limit is calculated to be as low as 15 nM according to the  $3\sigma/k$  method (Figure S5). The HRMS of the reaction solution between probe **NHF** and HClO ( $M^+=284.11536$ ) showed the formation of the MB dye ( $M^+=286.12159$ ) (Figure S6), which indicated that the detection mechanism is well agree with other reported literatures<sup>[14]</sup> (Scheme 1b).

To investigate the real-time detection ability of the probe, the time-dependent fluorescence spectra were respectively recorded after adding different concentrations of HClO. As shown in Figure 1c, probe **NHF** reacts with HClO very quickly. Even a small amount of HClO (0.3 equiv) can be accomplished almost instantaneously. Therefore, the probe could be used for monitoring HClO in real-time. The effect of pH on the fluorescence properties was also invulated. As shown in Figure 1d, probe **NHF** alone displayed almost constant intensity. After reaction with HClO (10 equiv), obvious fluorescent enhancement appeared in a broad pH range between 4.0 to 10.0. The above results indicated that probe **NHF** could be used for real-time detection of trace HClO in solution.

The specificity is an important parameter of the fluorescence probe. We further measured the fluorescence spectrum of probe **NHF** in the presence of different analysts. These analytes include cations ( $\text{Li}^+$ ,  $\text{K}^+$ ,  $\text{Mg}^{2+}$ ,  $\text{Ca}^{2+}$ ,  $\text{Zn}^{2+}$ ,  $\text{Cu}^{2+}$ ,  $\text{Al}^{3+}$ ,  $\text{Fe}^{3+}$ ,  $\text{Cr}^{2+}$ ,  $\text{Ba}^{2+}$ ,  $\text{Ag}^+$ ,  $\text{NH}_4^+$ ), anions ( $\text{F}^-$ ,  $\text{Cl}^-$ ,  $\text{Br}^-$ ,  $\text{I}^-$ ,  $\text{SO}_4^{2-}$ ,  $\text{S}_2\text{O}_3^{2-}$ ,  $\text{NO}_2^-$ ,  $\text{NO}_3^-$ ,  $\text{CO}_3^{2-}$ ,  $\text{Cr}_2\text{O}_7^{2-}$ ,  $\text{CH}_3\text{COO}^-$ ), the amino acid (Ala, Arg, Asn, Asp, Gln, Glu, Gly, His, Ile, Leu, Lys, Met, Phe, Pro, Ser, Thr, Trp, Tyr, Val), and reactive oxygen/nitrogen/sulfur species ( $\text{H}_2\text{O}_2$ ,  $\text{KO}_2$ ,  $t\text{-BuOOH}$ , NO,  $\text{ONOO}^-$ ,  $\text{SO}_3^{2-}$ , Cys, Hcy, GSH). As shown in Figure 2, except for HClO, various ions and amino acids do not influence the fluorescent properties of the probe **NHF** (Figure 2a-2c). Besides,  $\text{ONOO}^-$ , a kind of reactive nitrogen species having comparable oxidizability with HClO, does not interfere with the detection of HClO. Also, probe **NHF** can distinguish HClO over other analytes by naked eyes. In the presence of HClO, the color of the probe solution changed from colorless to blue (Figure 2e). The above results showed probe **NHF** exhibits excellent selectivity for HClO and can detect HClO with both colorimetric and fluorescent dual-channels.

**Cell selectivity of probe NHF.** The cytotoxicity of probe **NHF** was evaluated using standard MTT methods, and the results showed the cell viability is higher than 85% with the concentration of the probe below 40  $\mu\text{M}$  (Figure S7). The cell selectivity was further performed using four kinds of cell lines including HepG2 cells, HeLa cells, A549 cells, and GES-1 cells. As shown in Figure 3, all the cells displayed ignorable fluorescence by incubating with probe **NHF** alone for 1 h (Figure 3a). Further



**Figure 2.** The fluorescence intensity ( $F_{700\text{ nm}}$ ) of probe **NHF** ( $10\ \mu\text{M}$ ) towards various analysts. (a) Cations ( $100\ \mu\text{M}$ ): Lanes from 1 to 14: probe only,  $\text{Li}^+$ ,  $\text{K}^+$ ,  $\text{Mg}^{2+}$ ,  $\text{Ca}^{2+}$ ,  $\text{Zn}^{2+}$ ,  $\text{Cu}^{2+}$ ,  $\text{Al}^{3+}$ ,  $\text{Fe}^{3+}$ ,  $\text{Cr}^{2+}$ ,  $\text{Ba}^{2+}$ ,  $\text{Ag}^+$ ,  $\text{NH}_4^+$ ,  $\text{HClO}$  ( $10\ \mu\text{M}$ ); (b) Anions ( $100\ \mu\text{M}$ ): Lanes from 1 to 13: probe only,  $\text{F}^-$ ,  $\text{Cl}^-$ ,  $\text{Br}^-$ ,  $\text{I}^-$ ,  $\text{SO}_4^{2-}$ ,  $\text{S}_2\text{O}_3^{2-}$ ,  $\text{NO}_2^-$ ,  $\text{NO}_3^-$ ,  $\text{CO}_3^{2-}$ ,  $\text{Cr}_2\text{O}_7^{2-}$ ,  $\text{CH}_3\text{COO}^-$ ,  $\text{HClO}$  ( $10\ \mu\text{M}$ ). (c) Amino acids ( $100\ \mu\text{M}$ ): Lanes from 1 to 21: probe only, Ala, Arg, Asn, Asp, Gln, Glu, Gly, His, Ile, Leu, Lys, Met, Phe, Pro, Ser, Thr, Trp, Tyr, Val,  $\text{HClO}$  ( $10\ \mu\text{M}$ ). (d) Lanes from 1 to 13: probe only,  $\text{H}_2\text{O}_2$  ( $100\ \mu\text{M}$ ),  $\text{KO}_2$  ( $100\ \mu\text{M}$ ),  $t\text{-BuOOH}$  ( $100\ \mu\text{M}$ ),  $\text{NO}$  ( $100\ \mu\text{M}$ ),  $\text{ONOO}^-$  ( $100\ \mu\text{M}$ ),  $\text{SO}_3^{2-}$  ( $100\ \mu\text{M}$ ), Cys ( $1\ \text{mM}$ ), Hcy ( $1\ \text{mM}$ ), GSH ( $5\ \text{mM}$ ),  $\text{HClO}$  ( $1\ \mu\text{M}$ ),  $\text{HClO}$  ( $5\ \mu\text{M}$ ),  $\text{HClO}$  ( $10\ \mu\text{M}$ ). (e) Color changes of probe **NHF** ( $10\ \mu\text{M}$ ) after adding different analysts. All experiments were carried out in PBS buffer ( $20\ \text{mM}$ ,  $\text{pH}\ 7.4$ ) at room temperature for 5 min.

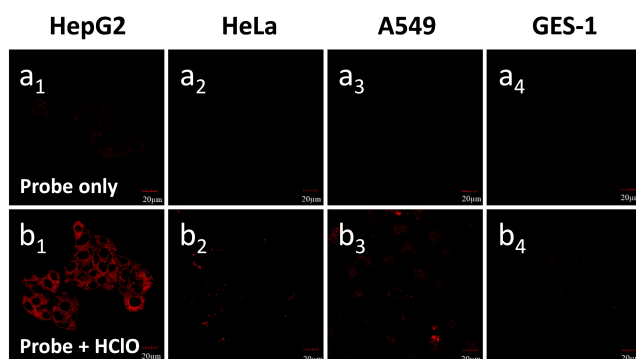


**Figure 3.** Fluorescence imaging of four kinds of cells incubated with probe **NHF** ( $10\ \mu\text{M}$ ) only for 1 h (a) and further treated with  $\text{HClO}$  ( $100\ \mu\text{M}$ ) for another 15 min (b).

treated with  $\text{HClO}$  for 15 min, obvious red fluorescence appeared in HepG2 cells. While the other three cells still showed weak or ignorable fluorescence. That is might be ASGPR is expressed most heavily in the surface of hepatocyte, GalNAc as the specific ligand for ASGPR facilitate targeted delivery to HepG2 cells.<sup>[16]</sup> Next, we further performed a competitive imaging experiment to confirm the mechanism of cell selectivity. Galactose was used as a competitive binding agent, which was pretreated to HepG2 cells for 30 min. As can be seen in Figure 4, red fluorescence in HepG2 cells decreased significantly

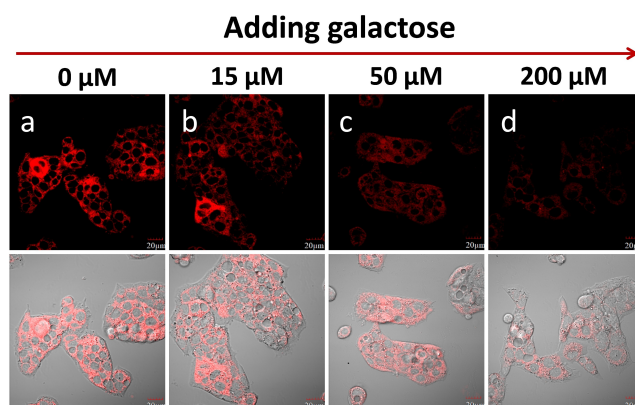


**Figure 4.** Fluorescence imaging of HepG2 cells incubated with **NHF** ( $10\ \mu\text{M}$ ) for 1 h and further  $\text{HClO}$  ( $100\ \mu\text{M}$ ) for another 15 min in the presence of different concentrations of galactose ( $0, 15, 50, 200\ \mu\text{M}$ ).

in a concentration-dependent manner. These imaging results implied that probe **NHF** could selectively transferred to HepG2 cells by specific interaction between GalNAc and ASGPR.

**Imaging of  $\text{HClO}$  in HepG2 cells.** We further investigated the imaging capability of the probe in HepG2 cells. As shown in Figure S8, the more  $\text{HClO}$  added, the brighter NIR fluorescence appeared, which implied probe **NHF** has good cell permeability and is responsive to exogenous  $\text{HClO}$  well in HepG2 cells.

During the liver transplantation, blood reflowing after a short-term hypoxic environment will induce the production of ROS, and the result is the ischemia-reperfusion injury (HIRI).  $\text{HClO}$ , one of the ROS, is an important mediator of inflammatory processes, which might be associated with HIRI.<sup>[17]</sup> To imaging endogenous  $\text{HClO}$  during HIRI, OGD/R model HepG2 cells were first established by cultured HepG2 cells in sugarless DMEM containing  $0.5\ \text{mM}$  sodium hydrosulfite for 30 min and then in high glucose DMEM for another 30 min.<sup>[18]</sup> As shown in Figure 5, probe **NHF** treated OGD/R HepG2 cells displayed brighter red fluorescence than the control cells. The above imaging results indicated that probe **NHF** could be used to image exogenous and endogenous  $\text{HClO}$ . Particularly worth mentioning is that the visualization of endogenous  $\text{HClO}$  during OGD/R in HepG2 cells using fluorescent probes has not been any reports so far.

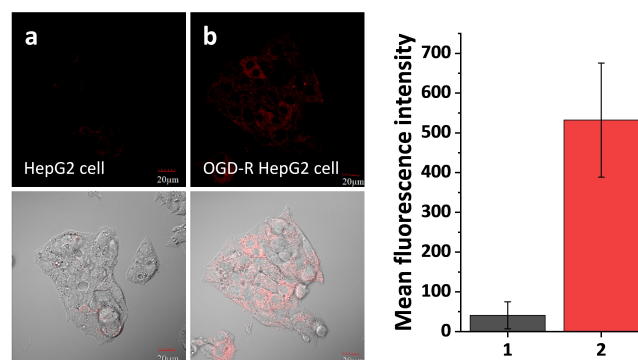


**Figure 5.** Fluorescence imaging of endogenous  $\text{HClO}$  in HepG2 cells (a) and OGD/R HepG2 cells (b). All cells were treated with probe **NHF** ( $10\ \mu\text{M}$ ) for 1 h.

We also observed LPS/PMA induced endogenous HCIO production in HepG2 cells (Figure S9).

**Imaging of HCIO *in vivo*.** Encouraged by the imaging capability in HepG2 cells, probe **NHF** was used to visualize HCIO *in vivo*. Zebrafish, a model animal, was first used for confocal fluorescence imaging studies. As shown in Figure 6, zebrafish incubated with probe **NHF** only for 1 h showed no fluorescence (Figure 6a), and very distinct red fluorescence was seen in the liver region of zebrafish after further treatment with HOCl (1.0 equiv) for 10 min (Figure 6b). While zebrafish cultured with GalNAc-free probe **CP** displayed divergent fluorescence in the liver and intestine (Figure S10). These results mean probe **NHF** can be targeted to the liver of zebrafish. Considering the drug metabolites may initiate an up-regulation of endogenous HCIO level,<sup>[19]</sup> we cultured zebrafish with acetaminophen (APAP), a commercial medicine used to relieve pain and fever, for 24 h, then treated with probe **NHF** for 1 h, obvious red fluorescence appeared in the liver of zebrafish (Figure 6c). The imaging

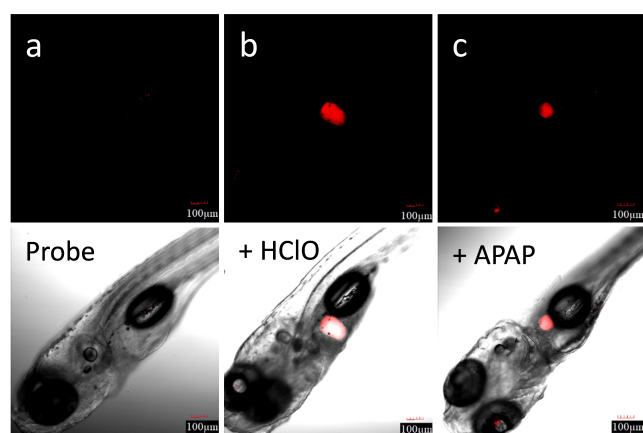


**Figure 6.** Fluorescence imaging of HCIO in zebrafish. Zebrafish were cultured with probe **NHF** (10  $\mu$ M) for 1 h (a) or further added with HCIO (10  $\mu$ M) for 10 min (b) or pretreated with APAP (1 mM) for 12 h (c) in the E3 culture medium.

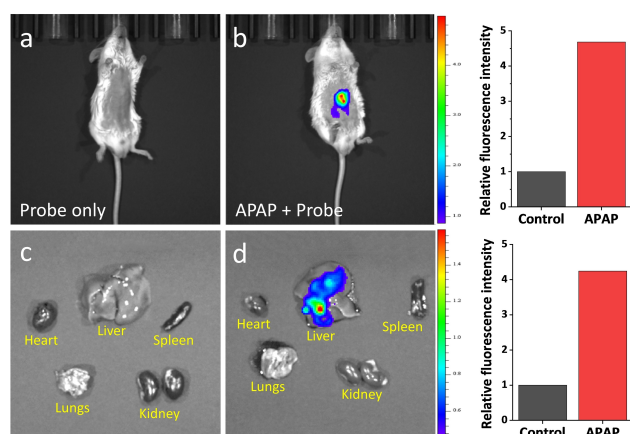


**Figure 7.** Fluorescence imaging of HCIO in mice (a, b) and the main organs of mice (c, d). Mice were injected with probe **NHF** (200  $\mu$ M, 100  $\mu$ L) only by i.v. injection for 15 min (a) or pre-incubated with APAP (300 mg/Kg) intraperitoneally for 8 h (b). (c, d) Main organs of mice in a and b (1: liver, 2: heart, 3: spleen, 4: lungs, 5: kidney).

results showed probe **NHF** can monitor the changes of exogenous and endogenous HCIO in the liver tissue in zebrafish.

To further demonstrate the application of the NIR probe, probe **NHF** was used to visualize HCIO in mice. Experimental mice were first injected with APAP intraperitoneally for 8 h to induce the up-regulation of endogenous HCIO, and then given an intravenous injection of probe **NHF**. The control mice were only treated via intraperitoneal injection of probe **NHF**. After reaction *in vivo* for 15 min, the mice were anesthetized for imaging. As can be seen in Figure 7b, the APAP pretreated mice showed clear fluorescence. Subsequently, the mice were sacrificed and the main organs were recovered (Figure 7c and 7d). The imaging is clear and proven that the selective localization of probe **NHF** is in the liver organ over other organs including the heart, spleen, lungs, and kidney. These imaging results indicated that probe **NHF** has good liver targeting ability. And it is also worth noting that NIR fluorescent probes for specific detection of HCIO in the liver *in vivo* are rarely reported. Probe **NHF** can be considered as an excellent tool for dynamic monitoring endogenous HCIO in the liver region *in vivo*.

## Conclusion

A novel NIR hepatocyte-specific fluorescent probe for HCIO was designed and synthesized. The probe can respond to trace HCIO in real time (<3 s) with large spectral variation in buffer solution. The probe was able to achieve hepatocyte by the highly specific interaction between GalNAc and ASGPR, and first visualized the up-regulation of endogenous HCIO in the OGD/R HepG2 cells. In particular, this NIR probe can be applied to dynamically monitor HCIO in the liver tissue of zebrafish and mice *in situ* during APAP treatment.

## Experimental Section

### Materials and instruments

All chemicals were purchased from innochem and J&K (Beijing, China). All other reagents were analytical grade and used without further purification. The UV-vis absorption spectra were recorded on an Agilent Cary-5000 spectrophotometer. Fluorescence measurements were operated on a Hitachi F-7000 spectrofluorimeter. <sup>1</sup>H NMR and <sup>13</sup>C NMR spectra were recorded on a Bruker AVANCE III 400 MHz spectrometer using *d*<sub>6</sub>-DMSO and CDCl<sub>3</sub> as the solvents. High-resolution mass spectra (HRMS) were obtained on a Bruker Fourier transform ion cyclotron resonance mass spectrometry. Fluorescence imaging of cells and zebrafish was carried out by an Olympus FV1000 confocal microscope. Fluorescence imaging of mice was performed on an IVIS Spectrum small animal optical *in vivo* imaging system.

### Synthesis of probe **NHF**

To the solution of GalNAc-NH<sub>2</sub> (96 mg, 0.30 mmol) and sodium carbonate (95 mg, 0.90 mmol) in 10 mL dry THF, compound 1

(104 mg, 0.30 mmol) in 5 mL dry THF was added dropwise. After stirring for 4 h at room temperature, the reaction solution was concentrated under reduced pressure. Probe **NHF** was obtained as a white solid via column chromatography (142 mg, yield 75%, dichloromethane/methanol=1/5). <sup>1</sup>H NMR (400 MHz, DMSO-*d*<sub>6</sub>) δ (ppm): 7.62 (d, *J*=9.2 Hz, 1H), 7.26 (d, *J*=4.4 Hz, 2H), 6.70 (s, 2H), 6.66 (d, *J*=8.8 Hz, 2H), 5.96 (s, 1H), 4.24 (d, *J*=8.4 Hz, 1H), 3.78–3.72 (m, 1H), 3.71 (t, *J*=9.6 Hz, 1H), 3.61 (s, 1H), 3.52–3.45 (m, 6H), 3.40–3.34 (m, 3H), 3.28 (t, *J*=6.4 Hz, 4H), 3.20–3.13 (m, 2H), 2.88 (s, 12H), 1.79 (s, 3H); <sup>13</sup>C NMR (101 MHz, DMSO-*d*<sub>6</sub>) δ (ppm): 170.1, 155.7, 149.0, 133.6, 128.7, 127.8, 111.7, 110.8, 101.9, 75.7, 71.9, 69.8, 69.7, 68.1, 67.8, 60.8, 55.4, 52.4, 40.7, 36.3, 23.6. HRMS (ESI, *m/z*): calculated for C<sub>29</sub>H<sub>41</sub>N<sub>5</sub>O<sub>8</sub>S [M]<sup>+</sup>, 619.2676, found 619.2676.

### General procedures for spectra measurements

All spectra were obtained in PBS (20 mM, pH=7.4). Probe **NHF** was dissolved in DMSO to prepare a 5 mM stock solution and used at 10 μM. The concentration of HClO was determined by the absorptive intensity at 292 nm. Other reactive species were prepared according to reported literature.<sup>[14b]</sup> The fluorescent spectra were excited at 620 nm and collected between 640 to 850 nm. The slide width for excitation and emission was 5.0 nm and 10.0 nm, respectively.

### Fluorescence imaging in living cells

Four kinds of cells including HepG2 cells, HeLa cells, A549 cells, and GES-1 cells were respectively cultured in DMEM at 37 °C in the 5% CO<sub>2</sub> atmosphere. For the cell selectivity imaging, the above cells were treated with galactose (0, 15, 50, 200 μM) for 30 min, then incubated with probe **NHF** (10 μM) for 1 h and finally with HClO (100 μM) for 15 min. For imaging exogenous HClO, HepG2 cells were first incubated with probe **NHF** (10 μM) for 1 h, then incubated with HClO (0, 50, 100 μM) for another 15 min. For imaging endogenous HClO in OGD/R model HepG2 cells were treated with probe **NHF** (10 μM) for 1 h. For imaging LPS/PMA induced endogenous HClO production, HepG2 cells were first treated with LPS (1 mg/mL<sup>-1</sup>) for 12 h and PMA (1 mg/mL<sup>-1</sup>) for 30 min and subsequent treatment with probe **NHF** (10 μM) only for 1 h. The confocal images were excited at 633 nm and collected between 650 to 750 nm.

### Fluorescence imaging in zebrafish

Zebrafish were purchased from Eze-Rinka Company (Nanjing, China) and cultured in E3 medium. Five day's old zebrafish were only incubated with **NHF** (10 μM) for 1 h as control, further treated with HClO (10 μM) for 10 min to image exogenous HClO. For monitoring endogenous HClO, zebrafish were treated with acetaminophen (APAP, 1 mM) and probe **NHF** (10 μM) for 24 h and 1 h, respectively. Confocal images were excited at 633 nm and collected between 650 to 750 nm.

### Fluorescence imaging in mice

The 5-week-old Kunming Mice (female) were purchased from Beijing Vital River Laboratory Animal Technology Co. Ltd. All operation were performed according to the guidelines by the ethical committee of Hebei University. Mice in the control group were peritoneal injection with PBS (200 μL), then probe **NHF** (200 μM, 100 μL) was given intravenously. In the experimental group, mice were peritoneal injection with APAP (300 mg/Kg, 200 μL) for 8 h, and then injected probe **NHF** (200 μM, 100 μL PBS) at the same

region. Fluorescence images were taken at 15 min after probe administration. The mice were then euthanized and their major organs (heart, liver, spleen, lungs, kidneys) were quickly removed for imaging. All images were excited at 665 nm.

### Acknowledgements

We sincerely thank Prof. Baoxiang Gao for his great support in confocal microscopy imaging. This work was supported by the Natural Science Foundation of Hebei Province (B2019201418, B2018201234), the Foundation of Hebei Education Department (QN2017015), and the Upgrading Program for Key Laboratory of Medicinal Chemistry and Molecular Diagnosis of Ministry of Education (Hebei University) (ts2020001).

### Conflict of Interest

The authors declare no conflict of interest.

**Keywords:** hypochlorous acid · near-infrared fluorescent · hepatocyte-specific probe · liver tissue · bioimaging

- [1] J. Sun, F. Feng, *Analyst* **2018**, *143*, 4251–4255.
- [2] Z. Lou, P. Li, K. Han, *Acc. Chem. Res.* **2015**, *48*, 1358–1368.
- [3] S. J. Klebanoff, A. J. Kettle, H. Rosen, C. C. Winterbourn, W. M. Nauseef, *J. Leukocyte Biol.* **2013**, *93*, 185–198.
- [4] D. A. Ford, *Clin. Lipidol.* **2010**, *5*, 835–852.
- [5] D. I. Pattison, M. J. Davies, *Biochemistry* **2006**, *45*, 8152–8162.
- [6] S. Sugiyama, Y. Okada, G. K. Sukhova, R. Virmani, J. W. Heinecke, P. Libby, *Am. J. Pathol.* **2001**, *158*, 879–891.
- [7] a) A. C. Maritim, R. A. Sanders, J. B. Watkins, *J. Biochem. Mol. Toxicol.* **2003**, *17*, 24–38; b) T. Hasegawa, E. Malle, A. Farhood, H. Jaeschke, *Am. J. Physiol. Gastrointest. Liver Physiol.* **2005**, *289*, G760–G767.
- [8] R. A. Roberts, D. L. Laskin, C. V. Smith, F. M. Robertson, E. M. Allen, J. A. Doorn, W. Slikker, *J. Toxicol. Sci.* **2009**, *112*, 4–16.
- [9] a) D. Wu, L. Chen, Q. Xu, X. Chen, J. Yoon, *Acc. Chem. Res.* **2019**, *52*, 2158–2168; b) Y.-R. Zhang, Y. Liu, X. Feng, B.-X. Zhao, *Sens. Actuators B* **2017**, *240*, 18–36; c) R. Zhang, B. Song, J. L. Yuan, *TRAC Trends Anal. Chem.* **2018**, *99*, 1–33; d) M. G. Ren, K. Zhou, L. W. He, W. Y. Lin, *J. Mater. Chem. B* **2018**, *6*, 1716–1733.
- [10] a) H. D. Xiao, J. H. Li, J. Zhao, G. Yin, Y. W. Quan, J. Wang, R. Y. Wang, *J. Mater. Chem. B* **2015**, *3*, 1633–1638; b) J. Han, Y. Li, Y. Wang, X. Bao, L. Wang, L. Ren, L. Ni, C. Li, *Sens. Actuators B* **2018**, *273*, 778–783; c) B. C. Zhu, P. Li, W. Shu, X. Wang, C. Y. Liu, Y. Wang, Z. K. Wang, Y. W. Wang, B. Tang, *Anal. Chem.* **2016**, *88*, 12532–12538; d) F. Ali, S. Aute, S. Sreedharan, H. A. Anila, H. K. Saeed, C. G. Smythe, J. A. Thomas, A. Das, *Chem. Commun.* **2018**, *54*, 1849–1852; e) C. Zhang, Q. Nie, I. Ismail, Z. Xi, L. Yi, *Chem. Commun.* **2018**, *54*, 3835–3838; f) L. He, H. Xiong, B. Wang, Y. Zhang, J. Wang, H. Zhang, H. Li, Z. Yang, X. Song, *Anal. Chem.* **2020**, *92*, 11029–11034; g) X. Wang, Y. Tao, J. Zhang, M. Chen, N. Wang, X. Ji, W. Zhao, *Chem. Asian J.* **2020**, *15*, 770–774; h) P. Lu, X. Zhang, T. Ren, L. Yuan, *Chin. Chem. Lett.* **2020**, *31*, 2980–2984; i) Y. Deng, S. Feng, Q. Xia, S. Gong, G. Feng, *Talanta* **2020**, *215*, 120901.
- [11] G. Zheng, Z. Li, Q. Duan, K. Cheng, Y. He, S. Huang, H. Zhang, Y. Jiang, Y. Jia, H. Sun, *Sens. Actuators B* **2020**, *310*, 127890.
- [12] a) G. H. Cheng, J. L. Fan, W. Sun, J. F. Cao, C. Hu, X. J. Peng, *Chem. Commun.* **2014**, *50*, 1018–1020; b) S. S. Ding, Q. Zhang, S. H. Xue, G. Q. Feng, *Analyst* **2015**, *140*, 4687–4693; c) H. D. Xiao, K. Xin, H. F. Dou, G. Yin, Y. W. Quan, R. Y. Wang, *Chem. Commun.* **2015**, *51*, 1442–1445; d) H. X. Zhang, J. Liu, C. L. Liu, P. C. Yu, M. J. Sun, X. H. Yan, J. P. Guo, W. Guo, *Biomaterials* **2017**, *133*, 60–69; e) B. B. Deng, M. G. Ren, X. Q. Kong, K. Zhou, W. Y. Lin, *Sens. Actuators B* **2018**, *255*, 963–969; f) H. J. Tong, Y. J. Zhang, S. N. Ma, M. H. Zhang, N. Wang, R. Wang, K. Y. Lou, W. Wang, *Chin. Chem. Lett.* **2018**, *29*, 139–142; g) C. Duan, M. Won, P.

- Verwilst, J. Xu, H. S. Kim, L. Zeng, J. S. Kim, *Anal. Chem.* **2019**, *91*, 4172–4178; h) Y.-J. Gong, M.-K. Lv, M.-L. Zhang, Z.-Z. Kong, G.-J. Mao, *Talanta* **2019**, *192*, 128–134; i) D. Shi, S. Chen, B. Dong, Y. Zhang, C. Sheng, T. D. James, Y. Guo, *Chem. Sci.* **2019**, *10*, 3715–3722; j) Y. Huang, Y. Zhang, F. Huo, Y. Liu, C. Yin, *Dyes Pigm.* **2020**, *179*, 108387; k) W. Zheng, J. Yang, Y. Shen, Y. Yao, G. Lv, S. Hao, C. Li, *Dyes Pigm.* **2020**, *179*, 108404.
- [13] a) Q. X. Duan, P. Jia, Z. H. Zhuang, C. Y. Liu, X. Zhang, Z. K. Wang, W. L. Sheng, Z. L. Li, H. C. Zhu, B. C. Zhu, X. L. Zhang, *Anal. Chem.* **2019**, *91*, 2163–2168; b) H. Zhang, Z. J. Li, M. Wang, T. R. Luo, L. Yi, J. Y. Wang, *Sens. Actuators B* **2019**, *279*, 102–110.
- [14] a) P. Wei, W. Yuan, F. F. Xue, W. Zhou, R. H. Li, D. T. Zhang, T. Yi, *Chem. Sci.* **2018**, *9*, 495–501; b) P. Wei, L. Liu, Y. Wen, G. Zhao, F. Xue, W. Yuan, R. Li, Y. Zhong, M. Zhang, T. Yi, *Angew. Chem. Int. Ed.* **2019**, *58*, 4547–4551; *Angew. Chem.* **2019**, *131*, 4595–4599.
- [15] a) Z. Guo, M. Wang, X. Li, X. Jia, X. Wang, P. Zhang, C. Wei, X. Li, *Chem. Commun.* **2020**, *56*, 14183–14186; b) M. Yao, X. Jia, M. Wang, X. Li, X. Wang, H. Qu, X. Li, C. Wei, *Dyes Pigm.* **2021**, *188*, 109151.
- [16] S. K. Mamidyala, S. Dutta, B. A. Chrnyk, C. Préville, H. Wang, J. M. Withka, A. McColl, T. A. Subashi, S. J. Hawrylik, M. C. Griffor, S. Kim, J. A. Pfefferkorn, D. A. Price, E. Menhaji-Klotz, V. Mascitti, M. G. Finn, *J. Am. Chem. Soc.* **2012**, *134*, 1978–1981.
- [17] M. Abu-Amara, S. Y. Yang, N. Tapuria, B. Fuller, B. Davidson, A. Seifalian, *Liver Transplant.* **2010**, *16*, 1016–1032.
- [18] W. Zhang, J. Liu, P. Li, X. Wang, S. Bi, J. Zhang, W. Zhang, H. Wang, B. Tang, *Biomaterials* **2019**, *225*, 119499.
- [19] X. Jiao, Y. Xiao, Y. Li, M. Liang, X. Xie, X. Wang, B. Tang, *Anal. Chem.* **2018**, *90*, 7510–7516.

Manuscript received: May 4, 2021

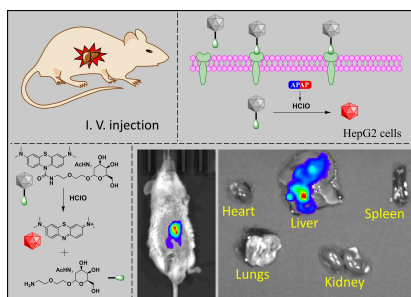
Revised manuscript received: May 22, 2021

Accepted manuscript online: May 25, 2021

Version of record online: ■■■, ■■■■

## FULL PAPER

A novel NIR hepatocyte-specific fluorescent probe was designed and synthesized for real-time visualization of the upregulation of endogenous HClO in the liver of zebrafish and mice in situ during APAP treatment.



X. Jia, Dr. C. Wei\*, Z. Li, L. Liu, Dr. M. Wang, Prof. Dr. P. Zhang, Prof. Dr. X. Li\*

1 – 7

Selective Imaging of HClO in the Liver Tissue In Vivo Using a Near-infrared Hepatocyte-specific Fluorescent Probe

